▌ Nanotechnology

Reversible Ultra-Slow Crystal Growth of Mixed Lead Bismuth Perovskite Nanocrystals: The Presence of Dynamic Capping

Shovon Chatterjee,[a] Pritam Dey,[b] Nilimesh Das,[a] Khushubo Tiwari,[c] Tanmoy Maiti,[b] and Pratik Sen*[a]

Abstract: An ultra-slow crystal growth over a period of 24 h of a newly synthesized $CH_3NH_3Pb_{1/2}Bi_{1/3}I_3$ perovskite (MPBI) nanocrystal in non-polar toluene medium is reported here. From several spectroscopic techniques as well as from TEM analysis we found that the size of nanocrystals changes continuously with time, in spite of being capped by the ligands. Using a single molecular spectroscopic technique, we also found that this size change is not due to the stacking of nanocrystals but due to crystal growth. The notable temperature dependence and reversible nature of the nanocrystals growth is explained by the dynamic nature of the capping. The observed temperature-dependent ultra-slow growth is believed to be a pragmatic step towards controlling the size of perovskite NC in a systematic manner.

Organic–inorganic hybrid perovskite materials of ABX_3 type with A as the organic cation, B as the inorganic cation and X as halide ions rendered appreciable interest to the scientific community due to their unique properties suitable for the construction of a photovoltaic cell with very high efficiency.[1–3] The nanocrystalline form of such perovskite materials showed a large fluorescence quantum yield with better photostability and considered to be a good replacement of the traditional chromophores.[4] The compositional tuning of such a nanocrystal (NC) provides well-tuned emission characteristics of the material that makes it a potential candidate in the field of optoelectronics, such as in lasers, nonlinear optics, and light emitting diodes.[5,6] Until now most of the reported perovskite NCs are lead (Pb)-based with high emission quantum yield.[7] Keeping in mind the toxic nature of lead, it is desired to develop

perovskite NCs with lower Pb content without compromising its interesting properties. Further, these Pb-based NCs exhibit poor moisture resistance, making these extremely vulnerable in the ambient conditions.[8] Recently scientists have started to explore Pb-free perovskites with various cations at the B-site.[9] Among these, bismuth (Bi) -based perovskites provide a better stability in the ambient condition, which is very much required for the application of these materials.[10] However, the quantum yield of these Bi-based perovskite NCs is very low.[11] Therefore, it is a primary concern to search for a system with high quantum yield without compromising stability. Keeping this in mind, we have synthesized organic–inorganic hybrid iodide perovskite NCs with an appropriate ratio of Pb^{2+} and Bi^{3+} in order to maintain the formal charge balance that is, $(+2)$ in the B-site of these perovskites. Properties of Bi-doped Pb halide NCs have been explored recently by some research groups.[12,13] In our previous study, we have also reported the potential of these charge-balanced hybrid Pb–Bi perovskite thin films for solar cell applications.[14]

Capping of NCs with long-chain organic moieties is a key step for size control synthesis of the NCs as without capping, the NCs stability is being compromised due to the formation of non-fluorescent bulk perovskite materials.[15] Thus, capping is one of the most efficient ways to enhance the stability of perovskite NCs in the solution[16–18] Oleic acid (OA) and oleylamine (OAm) are popular capping agents reported in the literature for the synthesis of such perovskite NCs.[15,16,18,19] OA has less capping ability than OAm, but any of these two alone cannot provide a sufficient stability to Pb perovskite NCs because of their poor binding with Pb^{2+}.[19] However, when these two ligands are used together, they form the oleate anion and olylammonium cation, which are better capping agents due to the strong interaction with Pb^{2+} and X^-, respectively.[15,19] For size and shape tunable synthesis of perovskite NCs, the proportion and the amount of OA and OAm play a crucial role. Akin to most of the nanomaterials, the properties of perovskite NCs depend highly on their size and shape.[16] With increase in the size of NCs, the emission maximum shifts towards lower energy, which can be controlled by the capping agents. Under controlled conditions, the spectral properties do not show any time dependence in most of the cases, rendering the formation of a stable NC.[5,6,15,16] Interestingly in one report, Seth et al. have demonstrated the time-dependent shift of the emission maxima for $CsPbBr_3$ and $CsPbBr_2I$ perovskite NC suspensions under continuous light irradiation.[20] To explain this phenomenon, the authors hypothesized a change in average size

[a] S. Chatterjee, N. Das, Prof. P. Sen
Department of Chemistry, Indian Institute of Technology Kanpur
Kanpur 208 016, UP (India)
E-mail: psen@iitk.ac.in

[b] P. Dey, Dr. T. Maiti
Plasmonics and Perovskites Laboratory, Department of
Materials Science and Engineering, Indian Institute of Technology Kanpur
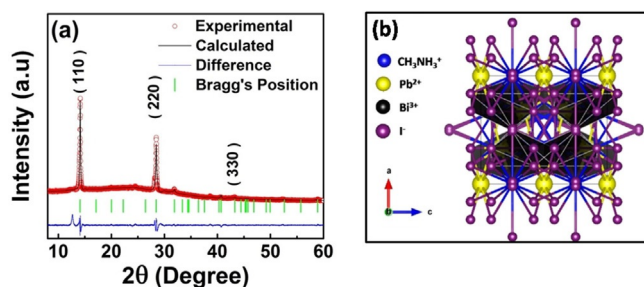Kanpur 208 016, UP (India)

[c] K. Tiwari
Department of Materials Science and Engineering; Indian Institute of
Technology Kanpur, Kanpur 208 016, UP (India)

📄 Supporting information and the ORCID identification number(s) for the
author(s) of this article can be found under:
https://doi.org/10.1002/chem.201904905.

of the NCs, though a detailed mechanism has not been put forward. Recently, Li et al. have reported a slow crystal growth of $CH_3NH_3PbBr_3$ perovskite NC on oil–water interface.[21] Kostopoulou et al. very recently reported a slow growth of $CsPbBr_3$ nanowire in toluene and a side to side coalescence of the nanocrystals is proposed as the mechanism.[22] However, to the best of our knowledge, such a slow crystal growth in normal antisolvent for hybrid perovskite NC has not been observed yet.

In the present study, we have developed a moisture-stable NC having both Pb and Bi at the B-site of the ABX_3 structure with chemical composition (MPBI) (refer to Section S1 of the Supporting Information). These NCs have shown greater stability compared to the pure Pb-based perovskite NCs. We have performed XRD analyses to find out the crystalline nature, XPS to verify the relative proportion of the individual components, and optical and microscopic characterizations (see Section S2 of the Supporting Information). Furthermore, we have observed a time-dependent emission phenomenon in toluene, which has been explained in terms of dynamic capping mediated crystal growth. To support our proposition, we have also carried out the temperature-dependent study to confirm the reversible nature of the dynamic capping process.

MPBI NCs have been synthesized through a single-step reaction by a ligand-assisted method.[16] The crystal structure of as-synthesized MPBI NCs has been determined by corrected XRD, which have been fitted using the LeBail method with constant scale factor in order to determine the lattice parameter and the space group (see Figure 1 a). It is evident that MPBI NCs have crystallized in a phase-pure tetragonal structure. The fitted data has been found to be consistent with tetragonal crystal symmetry with I4/mcm space group as shown schematically in Figure 1 b. Refined structural parameters of MPBI composition obtained by LeBail refinement of XRD data are as follows; $a = b = 8.86$ Å; $c = 10.353$ Å. From the XPS analysis we have shown the presence of Pb,Bi as well as iodine in the MPBI NCs. Detailed XPS analysis has been provided in Section S3 of the Supporting Information. In the UV/Visible spectra as demonstrated in Section S4, Figure S6 of the Supporting Information, MPBI NC suspension has shown a broad absorption spectrum and a strong emission centered at 579 nm at its stable condition after 24 h of the preparation with a maximum quantum yield of 10% at 25 °C (see Section S4, Figure S14 of the Supporting Information). An interesting feature of this study is

the time-dependent variation in the emission spectrum, in which one can see a huge redshift of 37 nm from the time zero spectrum ($\lambda_{em}^{max} = 542$ nm at 25 °C) (see Figure 2 d). The corresponding band edge is determined from the excitation spectra instead of absorption spectra because the absorption is very broad for such systems. The time-dependent excitation spectra also portray a clear redshift of band-edge position (see
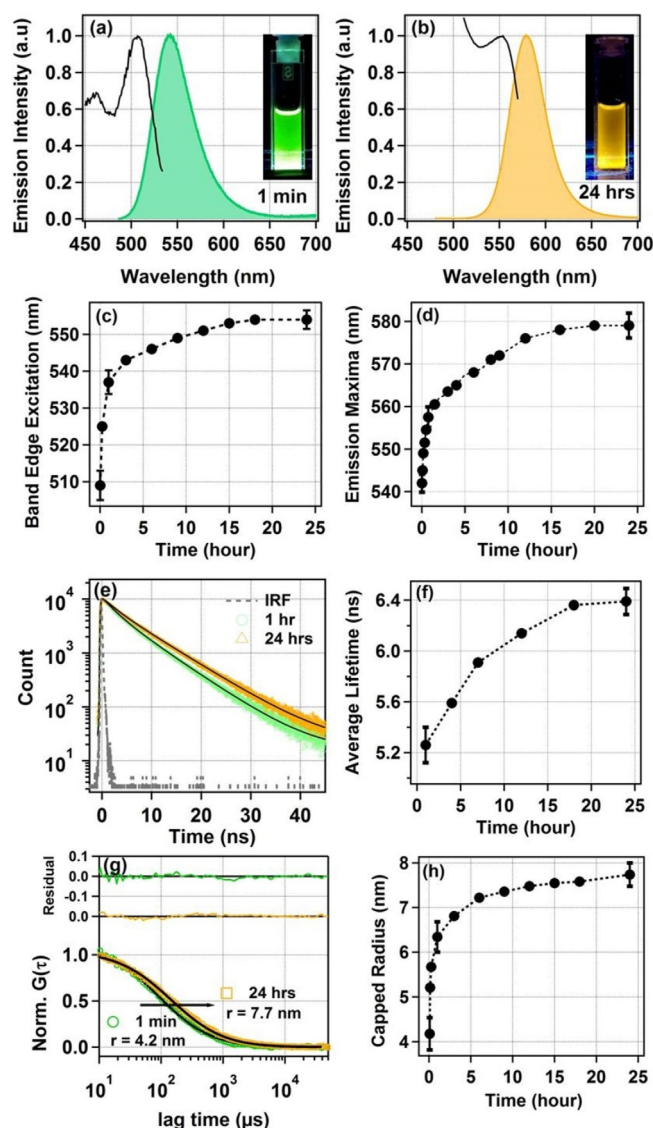

Figure 2. Time-dependent spectroscopic signals of MPBI NCs at 25 °C. (a) Emission spectra of MPBI NCs immediately after preparation (1 min) and corresponding excitation spectra. In the inset, the corresponding optical image of MPBI NC suspension under 365 nm UV light is shown. (b) Emission spectra of MPBI NCs after 24 h of its preparation and corresponding excitation spectra. In the inset, the corresponding optical image of MPBI NC suspension under 365 nm UV light is shown. (c) The change in band edge excitation maxima with time (excitation spectra are collected at corresponding emission maxima). (d) The change in emission maxima with time (excitation wavelength is 375 nm). (e) Fluorescent transients of MPBI NCs after 1 h (green circles, 558 nm) and after 24 h (yellow triangles, 578 nm) along with the best fit (black solid lines). Excitation wavelength is 375.8 nm. (f) The change in average lifetime with time. (g) FCS data of MPBI NCs immediately after preparation (1 min, green circles) and after 24 h (yellow squares) along with best-fit (black solid lines). (h) The change in capped radius value with time.

Figure 1. (a) Refined XRD data with Le-bail analysis. (b) Crystal model of MPBI.

Figure 2c and Section S4, Figure S9 of the Supporting Information). The red shift of the band edge as well as emission maxima may originate from the change in the size of the NC in the given time period. If so, this can be well explained by the quantum confinement.[23] In the strong quantum confinement regime, that is, when the size of the quantum dot is smaller than its excitonic Bohr radius then the effect of the size to the energy or band gap is much more pronounced.[23] In the strong confinement regime, a small increment in size attributes appreciably and results in a huge redshift in the emission maxima. This change in emission maxima as well as in the band-edge position of $CH_3NH_3PbI_3$ (MPI) NC was found to follow fast kinetics (see Figure S15c,e of Section S5 of the Supporting Information). The average fluorescence lifetime of MPBI also shows a similar trend as a function of time (see Figure 2e,f). The lifetime is found to be 5.3 ns at 1 h, which becomes 6.4 ns at 24 h and remains unaltered hence forth. Here, to note is that it has not been possible to measure the excited-state lifetime of the nanocrystal at an earlier time after its preparation, as the measurement of the lifetime takes about 20 min. The general perception on the photophysical characteristics of metal/semiconductor nanosystems is that the larger nanoparticles exhibit longer lifetime.[16, 24] The reason for this is not clear to us though. Nevertheless, in a similar line, we propose that the increase in the average lifetime is due to the increase in size of the MPBI NC with time. Fluorescence transients show a bi-exponential behavior with components of 2.6 and ≈ 7.0 ns for all the cases and interestingly, the contribution of the fast component decreases as a function of time until 24 h (see Section S4, Table S2 of the Supporting Information). The fast component is assigned to the bound exciton recombination process, which is formed immediately after the photoexcitation.[24] The longer component can be attributed to either trap-assisted recombination or diffused electron hole recombination.[25, 26] The diffused electron hole recombination process is itself a bimolecular process, which is favorable under high excitation power.[24] To confirm the origin of the longer time component we have performed the power-dependent component analysis (see Section S4, Figure S10 and Table S3 of the Supporting Information), which shows no excitation power dependence. Thus, we conclude that the slow time component is not due to bimolecular electron hole recombination and have assigned it to a trap-assisted recombination process.[25] It has been found that, the contribution of the slow component increases (62 % at 1 h to 76 % at 24 h) as the NCs size increases with time. Here another observation is that MPBI NC exhibits a shorter excited-state lifetime compared to pristine MPI NCs (see Figure S17 of Section S5 of Supporting Information).

To quantify the time-dependent growth of the MPBI NCs, we have further carried out fluorescence correlation spectroscopic (FCS) measurements. FCS is a very sensitive technique based on the temporal fluctuation of fluorescence intensity in a very small observation volume and provides a diffusion timescale of the emissive species. Mathematically, we get the diffusion timescale after fitting the autocorrelation curve, generated in the FCS experiments, with a single diffusion component equation. Then using the Stokes–Einstein relationship, the size of

the species can be calculated. The details of the experimental procedure, instrumentation and data fitting can be found in our previous publication as well as in the Section S2 of the Supporting Information.[27] The single component fitting suggests narrow distribution of NC sizes (see Figure 2g) and the calculated value of the radius of the NC is shown in Figure 2h. It is to be noted that in this case the measured size of the NC is actually the size of the capped NC as the diffusion of the NC is accompanied by its capping agents. The capped radius value is found to increase from 4.2 nm at 1 min to 7.7 nm at 24 h. The trend of the increase in size is found to correlate well with the shift in excitation band edge, emission maxima, and average lifetime (see Section S4, Figure S13 of Supporting Information for the comparison). This clearly indicates that the size modulation is the reason behind the observed change in the steady-state and time-resolved emission measurements. It suggests that the whole process is underway under the whole process is under quantum confinement regime.[23] A strong quantum confinement regime indicates that the NC size is smaller than Bohr excitonic diameter.[23] To confirm the measured size of the NC by the FCS method, we have taken the TEM images (Figure 3). Immediately after synthesis (1 min), after 1 h, and after 24 h, the diameters of the NCs are found to be 3, 7.5, and 9.5 nm, respectively (see Section S4, Figure S5 of the Supporting Information), which corroborates quite well with the measured value through FCS, after considering the size of the capping agents (see Section S6, Figure S18 of the Supporting Information). The almost spherical to somewhat irregular shapes of NCs in the TEM images also confirm the absence of any rod-shaped NCs, which can also induce a redshift to the emission maximum. From the HRTEM image of MPBI NCs after 24 h (Figure 3d), the crystal planes can be seen clearly. Figure 3e shows the Fourier filter image of the selected area from Figure 3c. As marked in lattice image, two types of planes, (220) and (222) with d-spacing of 0.354 and 0.262 nm, respectively, are observed. From this high-resolution imaging, we confirmed that the increase in size of the NCs is not due to agglomeration, but due to crystal growth. Figure 3f represents the diffraction pattern, which confirms the tetragonal crystal structure. To compare the growth kinetics of MPBI NCs with MPI NCs we performed time-dependent FCS measurement of MPI NCs, which renders a very fast increment in capped radius from 5.5 to 7.3 nm within an hour and remains same thereafter (Figure S15a, Supporting Information). For detailed growth kinetics of MPBI and MPI see Section S5 of the Supporting Information.

From all these investigations, we conclude that the size of the NC changes continuously with time and this increase in size originates through crystal growth of individual NCs and not through agglomeration of NCs. This is to note that the FCS studies are done in the nanomolar concentration and the possibility of agglomeration can be ruled out at this low concentration regime, which supports the HRTEM data. It is interesting to note here that even though the NCs are capped with OA and OAm, we could see a continuous growth. In most of the cases of perovskite NCs the emission maximum was found to be unaltered with time, although the intensity generally de-
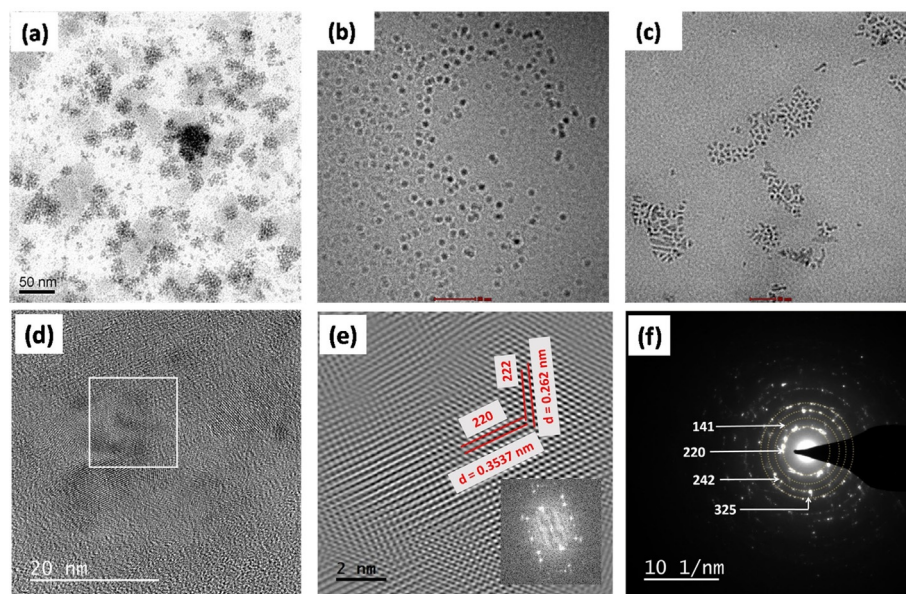
Figure 3. TEM images of MPBI NCs in toluene suspension (a) after 1 min of preparation, (b) after 1 h, and (c) after 24 h. (d) HRTEM image of MPBI NCs after 24 h. (e) Fourier filtered image of the selected area from Figure 3 d. The inset shows the FFT of the selected area. (f) Diffraction pattern of the MPBI NCs showing pure tetragonal crystal phase.

creases due to their stability issues.[10] The reason for the observed crystal growth may be explained by the improper capping of the NCs. It is plausible that if a sufficient amount of OA and OAm are not available to cap every individual NC then some of the NCs may have bare sites. To check this possibility, we have prepared the MPBI NCs using excess amounts of both OA and OAm, and also found a time-dependent redshift of the emission (Section S4, Figure S11 of the Supporting Information). However, in this case, the extent of shift is found to be smaller. This controlled experiment also proves that the observed shift in emission maxima is not the mere consequence of improper capping. Another reason for having a bare site on the NC surface even after proper capping is the dynamic nature of the capping, that is, the capping agents are in equilibrium between the free and capped state. Understandably, such an equilibrium should be affected by the temperature. If the dynamic capping is the reason for the observed time dependent change of the emission maximum of MPBI NCs, a decrease in the temperature should minimize the observed redshift with time. We have observed exactly the same as shown in Figure S11 of the Supporting Information. The observed red shift in the emission maximum after 24 h has been found to be 19 nm at 10 °C, compared to what has been 37 nm at 25 °C. Moreover, the proposition of the dynamic capping, that is, the existence of an equilibrium between the bound and free states of the capping agents, also suggests that even at the stable state of the NCs (e.g. after 24 h), a change in the temperature should also change the emission maximum of the NCs. From Figure 4 a,b, we can see that emission maxima of MPBI NCs exhibit high temperature dependence (553.5 nm at 5 °C to 581.2 nm at 30 °C) even after 24 h of its synthesis. The reversibility in temperature dependence also validates the presence of the equilibrium. FCS measurement also shows a decrease in size by lowering the temperature, which is reversible in nature

(see Figure 4 c,d). The schematic of the proposed equilibrium is shown in Figure 4 e. This is to note that the emission quantum yield of MPBI NCs decreases continuously from day 1 (Fig-
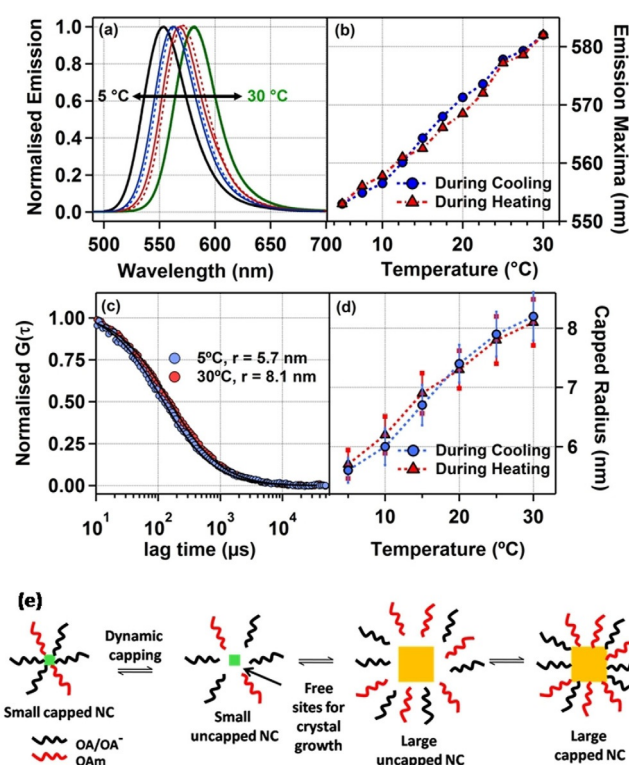
Figure 4. Temperature-dependent studies of MPBI NC after 24 hours from its preparation. (a) Reversible change of emission spectra with temperature. (b) The corresponding reversible change in emission maxima with temperature. (c) FCS data of MPBI NCs at 5 °C and at 30 °C. (d) Reversible change in capped radius with temperature. (e) Proposed mechanism of the crystal growth of MPBI NC in the toluene suspension mediated by dynamic capping.

ure S14 b of the Supporting Information), while the Stokes shift remains almost unaltered (see Section S5 of the Supporting Information). Thus we conclude that the observed decrease in the emission quantum yield is not likely to be due to the formation of any in-gap trapped state due to polaron defect.[28] Herein, we propose that the decrease in quantum yield may be due to partial degradation of the nanocrystal along with the surface ligand desorption followed by the generation of surface trap states, which leads to the formation of observed non-emissive MPBI precipitate.

In summary, we have synthesized a novel organic–inorganic hybrid lead-bismuth iodide perovskite NC, with charge balanced at the B-site of ABX_3 perovskite architecture, with a chemical composition of $CH_3NH_3Pb_{1/2}Bi_{1/3}I_3$ (MPBI). This NC is found to be stable for more than 7 days under ambient conditions (see Figure S2 of and Section S5 of the Supporting Information). MPBI NCs exhibit fairly strong emission characteristics with a maximum fluorescence quantum yield of 15%, which depends on the condition. The MPBI NCs are found to undergo an ultra-slow crystal growth until 24 h of its preparation and size remains unaltered thereafter. Such an ultra-slow crystal growth of perovskite NCs is very rare and to the best of our knowledge this is the first report of hybrid perovskite NC growth in a normal anti-solvent medium. In addition, by controlling the temperature we can tune the extent of crystal growth. We believe that the present work is an important advancement towards controlling the perovskite NC size in a systematic manner. In future studies, we aim to arrest the crystal growth at any time point using external perturbation. We have also demonstrated that its spectral properties vary along with its size. Through the observed reversibility in the temperature-dependent emission and FCS measurement, the mechanism of the NC growth is explained in terms of dynamic capping. Just to emphasize here that in this report we have used FCS to measure the size of the NC for the very first time. MPBI NC is proposed to be a new category in the field of perovskite material, which can be a potential candidate for the replacement of pure lead-based perovskites.

Experimental Section

General

Experimental details are provided in the Supporting Information, which includes details of the MPBI preparation, instruments and techniques, material and optical characterizations and also a note on the correlation of the size of NCs from FCS and from TEM analysis.

Acknowledgements

Conflict of interest

The authors declare no conflict of interest.

[1] N. J. Jeon, J. H. Noh, W. S. Yang, Y. C. Kim, S. Ryu, J. Seo, S. I. Seok, *Nature* **2015**, *517*, 476.
[2] D. Li, P. Liao, X. Shai, W. Huang, S. Liu, H. Li, Y. Shen, M. Wang, *RSC Adv.* **2016**, *6*, 89356.
[3] Q. Fu, X. Tang, B. Huang, T. Hu, L. Tan, L. Chen, Y. Chen, *Adv. Sci.* **2018**, *5*, 1700387.
[4] M. Gao, C. Zhang, L. Lian, J. Guo, Y. Xia, F. Pan, X. Su, J. Zhang, H. Li, D. Zhang, *J. Mater. Chem. C* **2019**, *3*, 3688.
[5] Y. Zhao, K. Zhu, *Chem. Soc. Rev.* **2016**, *45*, 655.
[6] H. Fu, *J. Mater. Chem. A* **2019**, *7*, 14357.
[7] J. Shamsi, A. S. Urban, M. Imran, L. D. Trizio, L. Manna, *Chem. Rev.* **2019**, *119*, 3296.
[8] Y. Dong, Y. Zhao, S. Zhang, Y. Dai, L. Liu, Y. Li, Q. Chen, *J. Mater. Chem. A* **2018**, *6*, 21729.
[9] J. Sun, J. Yang, J. I. Lee, J. H. Cho, M. S. Kang, *J. Phys. Chem. Lett.* **2018**, *9*, 1573.
[10] B. Yang, J. Chen, F. Hong, X. Mao, K. Zheng, S. Yang, Y. Li, T. Pullerits, W. Deng, K. Han, *Angew. Chem. Int. Ed.* **2017**, *56*, 12471; *Angew. Chem.* **2017**, *129*, 12645.
[11] M. Leng, Z. Chen, Y. Yang, Z. Li, K. Zeng, K. Li, G. Niu, Y. He, Q. Zhou, J. Tang, *Angew. Chem. Int. Ed.* **2016**, *55*, 15012; *Angew. Chem.* **2016**, *128*, 15236.
[12] R. Begum, M. R. Parida, A. L. Abdelhady, B. Murali, N. M. Alyami, G. H. Ahmed, M. N. Hedhili, O. M. Bakr, O. F. Mohammed, *J. Am. Chem. Soc.* **2017**, *139*, 731.
[13] H. Shao, X. Bai, H. Cui, G. Pan, P. Jing, S. Qu, J. Zhu, Y. Zhai, B. Dong, H. Song, *Nanoscale* **2018**, *10*, 1023.
[14] P. Dey, V. Khorwal, P. Sen, K. Biswas, T. Maiti, *ChemistrySelect* **2018**, *3*, 794.
[15] S. Seth, A. Samanta, *Sci. Rep.* **2016**, *6*, 37693.
[16] L. Levchuk, P. Herre, M. Brandl, A. Osvet, R. Hock, W. Peukert, P. Schweizer, E. Spiecker, M. Batentschuk, C. J. Brabek, *Chem. Commun.* **2017**, *53*, 244.
[17] Y. Tan, Y. Zou, L. Wu, Q. Huang, D. Yang, M. Chen, M. Ban, C. Wu, T. Wu, S. Bai, T. Song, Q. Zhang, B. Sun, *ACS Appl. Mater. Interfaces* **2018**, *10*, 3784.
[18] H. Xia, S. Wu, L. Li, S. Zhang, *RSC Adv.* **2018**, *8*, 35973.
[19] H. Huang, J. Raith, S. V. Kershaw, S. Kalytchuk, O. Tomanec, L. Jing, A. S. Susha, R. Zboril, A. L. Rogach, *Nat. Commun.* **2017**, *8*, 996.
[20] S. Seth, N. Mondal, S. Patra, A. Samanta, *J. Phys. Chem. Lett.* **2016**, *7*, 266.
[21] F. Li, L. Cao, S. Shi, H. Gao, L. Song, C. Geng, W. Bi, S. Xu, *Angew. Chem. Int. Ed.* **2019**, *58*, 17631; *Angew. Chem.* **2019**, *131*, 17795.
[22] A. Kostopoulou, M. Sygletou, K. Brintakis, A. Lappas, E. Stratakis, *Nanoscale* **2017**, *9*, 18202.
[23] J. Butkus, P. Vashishtha, K. Chen, J. K. Gallaher, S. K. K. Prasad, D. Z. Metin, N. Gaston, J. E. Halpert, J. M. Hodgkiss, *Chem. Mater.* **2017**, *29*, 3644.
[24] F. Di Stasio, M. Imran, Q. A. Akkerman, M. Prato, L. Manna, R. Krahne, *J. Phys. Chem. Lett.* **2017**, *8*, 2725.
[25] F. Zhang, H. Zhong, C. Chen, X. Wu, X. Hu, H. Huang, *ACS Nano* **2015**, *3*, 4533.
[26] V. A. Hintermayr, A. F. Richter, F. Ehrat, M. Döblinger, W. Vanderlinden, J. A. Sichert, Y. Tong, L. Polavarapu, J. Feldmann, A. S. Urban, *Adv. Mater.* **2016**, *28*, 9478.
[27] N. Das, P. Sen, *Biochemistry* **2018**, *57*, 6078.
[28] P.-P. Sun, D. R. Kripalani, L. Bai, K. Zhou, *J. Phys. Chem. C* **2019**, *123*, 12684.